

Lung imaging: how to get better look inside the lung

Lorenzo Ball, Veronica Vercesi, Federico Costantino, Karthikka Chandrapatham, Paolo Pelosi

Department of Surgical Sciences and Integrated Diagnostics, University of Genoa, Ospedale Policlinico San Martino-IRCCS per l'Oncologia, Genoa, Italy

Contributions: (I) Conception and design: L Ball, P Pelosi; (II) Administrative support: None; (III) Provision of study materials or patients: None; (IV) Collection and assembly of data: None; (V) Data analysis and interpretation: None; (VI) Manuscript writing: All authors; (VII) Final approval of manuscript: All authors.

Correspondence to: Professor Paolo Pelosi. Department of Surgical Sciences and Integrated Diagnostics, University of Genoa, Ospedale Policlinico San Martino-IRCCS per l'Oncologia, Largo Rosanna Benzi 8, Genoa 16131, Italy. Email: ppelosi@hotmail.com.

Abstract: In the last years, imaging has played a key role in the diagnosis and monitoring and critical illness, including acute respiratory distress syndrome (ARDS). Chest X-ray (CXR) and computed tomography (CT) are the conventional techniques most performed in the critically ill patients, the latter being the gold standard to assess lung aeration in ARDS patients. In addition, two bedside techniques are now gaining popularity alongside the conventional ones: lung ultrasound (LUS) and electrical impedance tomography (EIT). These techniques do not involve the use of ionizing radiations, are non-invasive and relatively easy to use, and are under extensive investigation as a complement, and for some application a substitution of conventional techniques. At last, positron emission tomography (PET) and magnetic resonance imaging (MRI) can provide functional information on the lung and respiratory function, and are increasingly used in research to improve the understanding of the pathophysiological mechanisms underlying ARDS. The purpose of this review is to give an up-to-date overview of the conventional and emerging imaging techniques available the diagnosis and management of patients with ARDS.

Keywords: Acute respiratory distress syndrome (ARDS); chest X-ray (CXR); computed tomography (CT); lung ultrasound (LUS); electrical impedance tomography (EIT); positron emission tomography (PET); magnetic resonance imaging (MRI)

Submitted Jul 01, 2017. Accepted for publication Jul 05, 2017.

doi: 10.21037/atm.2017.07.20

View this article at: <http://dx.doi.org/10.21037/atm.2017.07.20>

Introduction

Acute respiratory distress syndrome (ARDS) is a complex clinical entity, and since its first definition imaging had a key role in identifying its hallmark: bilateral lung infiltrates. In the last decades, several definitions of ARDS were proposed until the current Berlin definition (1), all of them comprising imaging as a diagnostic criterion. Nonetheless, both conventional and emerging imaging techniques had a dramatic technological improvement and were extensively studied in ARDS patients both for diagnosis and for monitoring the effects of therapy or the clinical evolution. A recent large observational trial reported an incidence of ARDS around 10%, with a relevant proportion not correctly

identified as such: this suggest that an improvement of the diagnostic process, including imaging, is still warranted (2).

The purpose of this review is to provide a comprehensive overview of the role of different imaging techniques in the diagnosis and management of ARDS patients.

Conventional imaging techniques

Two techniques have a predominant role in the current clinical practice, for their ease of use, widespread availability and on which most of the evidence concerning ARDS have been built: chest X-ray (CXR) and computed tomography (CT), either evaluated clinically or quantitatively, based on

the computer-based analysis of the acquired images. This paragraph illustrates the role of these two conventional techniques.

CXR

When heart failure is excluded or at least not fully explanatory of the respiratory failure, the presence of bilateral, homogenous or inhomogeneous and diffuse infiltrates observed on the frontal CXR is evocative of fluid accumulation around the alveolar barrier (3). This characteristic imaging pattern corresponds to one of the typical anatomopathological signs of ARDS, that together with hyaline membrane constitutes the diffuse alveolar damage (4). Usually, three or more lung lobes are involved in this inflammatory process, therefore the low specificity of CXR results in a laborious differential diagnosis with other, often overlapped, pulmonary conditions such as pneumonia, atelectasis and pleural effusion. In fact, the Berlin definition underlines the low sensitivity and specificity of CXR to evaluate the amount of non-cardiogenic interstitial oedema (1). The course of ARDS is divided in three phases, that could have corresponding CXR findings, even if the distinction between them is not always simple (5): acute, intermediate and late (6).

During the acute phase, within 48 h from onset, CXR could not show any pathological sign, after then a rapid worsening occurs, and diffuse bilateral opacities appear as 'white lung' image (*Figure 1A*); moreover, alveolar bronchograms and atelectasis are a frequent finding. In this phase, lung volumes are dramatically reduced and start posing a serious challenge for mechanical ventilation. For a specific radiologic diagnosis, the CXR should not show sign of heart failure such as heart shape enlargement, septal lines and pleural effusion: a comprehensive clinical evaluation is mandatory to perform an accurate differential diagnosis. In the intermediate or proliferative phase, occurring within 1–2 weeks from ARDS onset, the CXR aspect stabilizes presenting usual asymmetric consolidation and persistent diffuse infiltrates. At this stage, the lung tissue is prone to initiate a fibrotic degeneration process. The late or fibrotic phase is the most variable phase, influenced by intra- and inter-patient factors that can heavily affect the clinical outcome. In a widely variable interval of time, radiologic findings tend to improve, and the complete lung damage resolution depends on the severity of the ARDS, along with the patient's response, underlying condition and

comorbidities. The lung matrix is characterized by fibroblast proliferation as reaction to persistent inflammation, CXR may show a focal or a diffuse reticular pattern that usually corresponds to an increased physiological dead space. ARDS can resolve completely or progress to irreversible fibrosis: CXR will either show a *restitutio ad integrum* or a typical fibrotic pattern (*Figure 1B*).

Despite this formal classification, the correct interpretation of CXR in ARDS patients remains challenging. In fact, there is no univocal, reproducible and reliable method to recognize and define ARDS severity with CXR only. Researchers tried to validate against CT different scores to quantify interstitial lung oedema at the CXR (7), but their use in the current clinical practice is limited, as the reproducibility of these scores has been questioned, especially in case of focal loss of aeration (8). Nonetheless, bedside CXR is almost daily performed in ICU also nowadays, for other purposes than monitoring ARDS evolution, as it is inexpensive, widely available and undoubtedly useful for the detection of secondary complications such as pneumothorax and displacement of devices (9). Nevertheless, sensitivity and specificity power of CXR is lower compared to CT: for instance, when used to determine level of recruitment at different levels of PEEP, it has a major issue: the antero-posterior regions of the lung are merged, devices and technical images acquisition can limit the correct recruitment evaluation (10).

In conclusion, CXR is a still widely performed, fast, non-invasive and bed-side technique particularly useful to detect unpredictable acute conditions and device-related complications. Nonetheless, if used as a monitoring tool frequent exposure to ionizing radiations can be a concern, without guaranteeing high sensitivity and specificity, especially in the earlier stages (11).

CT

CT has profoundly changed the understanding of the pathophysiological processes underlying ARDS (12), and contributed to a better description of the topographic distribution of the loss of aeration.

CT can both be assessed visually, as typically done by radiologists, or quantitatively with computer-based analysis. In fact, CT creates an image in which each volume element (voxel) is attributed a value corresponding to its ability to attenuate X-rays, and it is normalized to a standard scale [Hounsfield units (HU)], in which -1,000 and 0 correspond

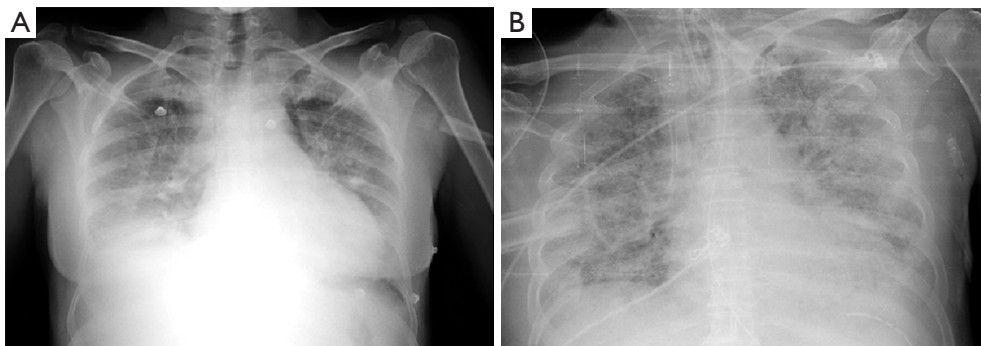


Figure 1 Chest X-ray of two patients with ARDS. (A) Patient with a severe ARDS in early phase, during non-invasive ventilation; (B) patient with a late fibrotic pattern in the context of a severe ARDS. ARDS, acute respiratory distress syndrome.

to air and water attenuation, respectively. Attenuation mainly depends on the atomic number of chemical elements composing the biological tissue, therefore, given a specific organ in which the elemental composition is substantially stable, such as occurs in lungs, HU can provide a reliable estimate of tissue density, expressed as grams per millilitre (13). Lung in ARDS is studied with a two-compartment model, assuming voxel density as the weighted average between tissue density (0 HU) and gas density (-1,000 HU). Lung weight can be estimated multiplying density and volume, and arbitrary thresholds have been defined to distinguish hyper-, normally-, poorly- and non-aerated lung tissue.

One of the first fields of application of CT was the assessment of PEEP effects in terms of lung recruitment, namely the amount of lung tissue that is re-aerated due to an increase in airway pressures (14). Nowadays, CT remains the gold standard imaging technique to evaluate aeration in ARDS patients and it is used to validate emerging imaging techniques (15). CT gave a major contribution to the development of the ‘baby lung’ concept: this functional entity, whose size is related to ARDS severity, is the portion of the lung parenchyma still physiologically aerated without collapsed or hyperinflated areas, therefore the smaller the ‘baby lung’, the lower the lung compliance (16). This concept provided a pathophysiological rationale for the use of low tidal volume ventilation (17), and PEEP to maintain the patency of respiratory units (18).

The most common CT finding in ARDS is the presence of large infiltrates and loss of aeration especially in the dorsal dependent regions (*Figure 2*). Compared to CXR, CT allows a more precise assessment of the morphology and distribution of the lesions, nonetheless ARDS has a

broad spectrum of radiological manifestations, therefore differential diagnosis with other lung conditions can still be complex. In the late phase, CT detects precisely the possible evolution of lung damage: patients who survived after severe ARDS can show a honeycomb-like pattern, indicating an irreversible fibrosis with restrictive syndrome. Concerning ARDS ventilatory management, CT can be useful to assess the degree of recruitment potential, namely the responsiveness to higher PEEP levels (19), the concept of ventilation titration based on imaging has been then proposed (20). Several studies assessed the responsiveness to recruiting by performing two or more CT scans during breath-hold at different PEEP levels, e.g., 5 vs. 45 cmH₂O (19,21). However, it has still to be demonstrated that setting PEEP according to imaging can improve the clinical outcome.

However, higher PEEP levels could keep open the dependent lung areas but also cause hyperinflation and consequently barotrauma in the aerated ones. In a recent paper, opening pressures were higher than what is commonly considered safe especially in moderate and severe ARDS (22): the clinician must therefore balance between the risk of lung de-recruitment and atelectrauma and that of volutrauma (23). Moreover, CT acquisition parameters can affect the quantitative analysis, especially for the quantification of the hyper-aerated lung tissue (24).

CT has important pitfalls, mainly the difficulties of the transport of critically ill patients from the ICU to the radiology facility, the exposure to a high dose of ionizing radiations and the long post-processing time required to perform quantitative analysis (15). The following section illustrates several experimental protocols that were proposed to overcome the latter two issues.

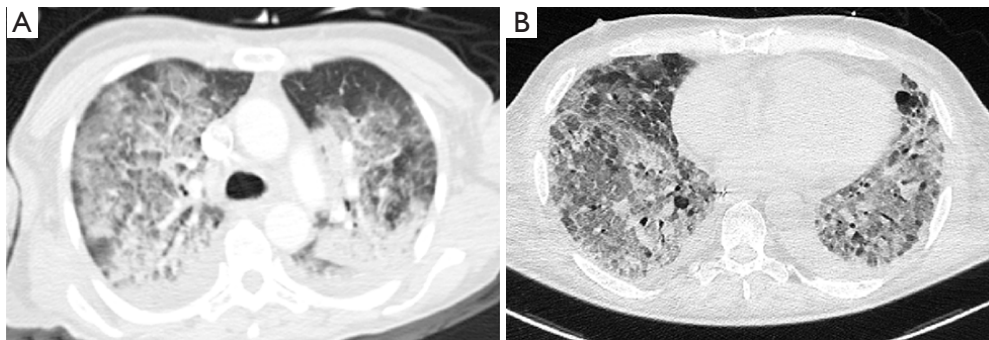


Figure 2 Computed tomography of two patients with ARDS. (A) Patient with a severe ARDS in early phase, showing diffuse bilateral infiltrates and small dorsal consolidated areas; (B) patient with a fibrotic pattern developed in the late phase of an ARDS, showing diffuse infiltrates with areas of ‘honeycomb’ pattern and left pleural effusion. The scans were obtained on the same patients and same day as in *Figure 1*. ARDS, acute respiratory distress syndrome.

Experimental CT acquisition protocols

For the purpose to reduce the workload to estimate lung aeration two methods have been proposed: extrapolation of a sub-set of ten slices from a whole-chest CT scan (25), and visual instead of computer-based image assessment (21). Concerning dose exposure reduction, low-dose spiral CT protocols with a reduced tube current have been tested (26), while more recently a protocol tried to combine low current tube with prospective acquisition of a reduced number of thin slices (27). All these strategies showed good concordance with the aeration assessment performed with conventional whole-chest CT scan, and could be useful to widen the clinical and research application of CT, especially when multiple scans are required, as is the case when recruitment is assessed performing the CT scan at two levels of PEEP. *Table 1* (21,22,25-30) compares the main characteristics of these experimental protocols.

In conclusion, CT has still nowadays an unreplaceable role in the study and clinical management of ARDS. Technology advances in new emerging bedside techniques could make it avoidable in the future. The availability of low-dose scanning protocols could be a compromise to increase the clinical applicability of CT and quantitative CT.

Emerging imaging techniques at the bedside

In addition to CXR and CT, that have gained a consolidated role in the diagnostic and management of ARDS patients, two other techniques are emerging for their ability to assess lung aeration at the bedside without using ionizing

radiation: the lung ultrasound (LUS) and electrical impedance tomography (EIT).

LUS

The use of transthoracic ultrasound has been confined for many years to the study of cardiovascular structures: the combination between air acoustic impedance and the intense ultrasound reflection, arising from the bone-lung parenchymal interface, produces massive reverberations effects, making the anatomical visualization of healthy lung impossible (31). The presence of exudate, transudate, collagen and blood changes the lung tissue’s density through a reduction of the air content, decreasing the acoustic mismatch with the surrounding tissues. As a consequence, the ultrasound beam can be partly reflected at deeper regions in injured lungs (32). The comprehension of the typical artefactual signs of lung sonographic imaging and the recurrence of specific patterns have contributed to a growing interest about LUS. We now witness the constitution of a more coherent body of evidence on this technique and international guidelines (ICC-LUS) have been developed concerning the use and limitations of LUS in the clinical practice (33).

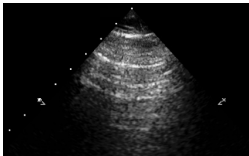
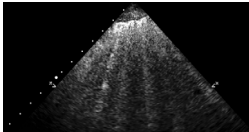
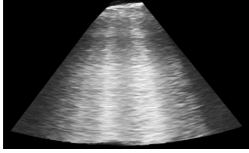
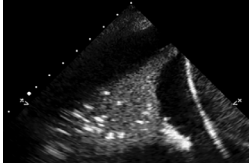
With LUS, clinicians can recognize ribs, pleural movement as the sliding of two regular lines corresponding to the pleural sheets, pulse determined by the transmission of heartbeat to the pleura and parenchymal reverberation artifacts or consolidated parenchyma. Lung aeration status can be summarized in four different echo patterns (*Table 2*). The extension of B-pattern images in the chest

Table 1 Protocols proposed for the reduction of either dose exposure or operator workload for quantitative or semi-quantitative lung aeration assessment in ARDS

Method	Description	Irradiated portion of the chest	Number of slices used in the analysis	Validation	Estimated dose reduction	Limitations
Retrospective extrapolation of slices (25)	Extrapolation of 10 equally spaced slices	Whole chest	10	Retrospective (157 critically ill patients, 41 ponies, 23 pigs, 11 sheep)	NA	No dose reduction
Low dose spiral CT (26)	Spiral scans at 60 and 30 mAs	Whole chest	30–40, 5 mm-slices	Prospective (45 patients with ARDS at two PEEP levels, 14 sheep)	–70% with 30 mAs	No reduction of number of slices
Visual assessment (21)	Visual estimation of recruited lung tissue at two PEEP levels	Whole chest	30–40, 5 mm-slices	Retrospective (50 patients with ARDS, scans performed at two PEEP levels)	NA	No dose reduction
Ultra-low dose sequential CT (27)	Thin-slice sequential scan performed with 180 and 50 mAs	1 mm portions interleaved by 20 mm of non-irradiated chest	10–12, 1 mm-slices	Prospective (12 pigs), retrospective (32 critically ill patients)	–97% with 50 mAs	Longer acquisition time

ARDS, acute respiratory distress syndrome; PEEP, positive end-expiratory pressure; CT, computed tomography; NA, not applicable.

Table 2 Lung ultrasound patterns and corresponding clinical interpretation

Pattern	Image	Findings	Interpretation
A		Reverberation artefacts parallel to the pleural line (A-lines)	Expression of a physiologically aerated lung when accompanied by the sliding sign of the pleural layers, but could also be present in hyper-inflated regions—normal lung aeration
B1		Multiple vertical artefacts (B-lines)	Correlated to extra vascular lung water content, absent in normal lung, hallmark of the alveolo-interstitial syndrome—moderate loss of aeration
B2		Multiple, coalescent B-lines	Further progression of the B1 pattern—severe loss of aeration
C		Real image, not artefact with tissue-like echogenicity, or shred sign (typical of alveolar consolidation)	Visible when consolidations are extended to the pleura—collapsed or consolidated lung tissue

correlates with the presence of interstitial syndrome as detected by CT scan (34), and also with the amount of extravascular lung water measured with transpulmonary thermodilution (35).

LUS can help the clinician in the diagnosis of ARDS, but, the mere presence of B-pattern images bilaterally is not specific as it cannot distinguish between ARDS and other diseases characterized by a sonographic image of interstitial syndrome as cardiogenic pulmonary oedema. Nonetheless, the ICC-LUS agrees that the presence of diffuse and inhomogeneous distribution of B lines, characterized by preserved and affected areas with different degrees of severity, associated with pleural line abnormalities and the reduction or absence of pleural sliding, accompanied by sub-pleural and/or pulmonary consolidations especially in frontal areas, is strongly indicative for ARDS (33,36). Nonetheless, a recent observational study proposed a modification of the Berlin criteria replacing arterial blood gas analysis and conventional imaging with pulse oximetry plus LUS, which could be of particular interest in low-resource settings (37).

A concomitant echocardiographic examination can be of help in the differential diagnosis, providing important information about the cardiac function, pulmonary hypertension, diameter of cava vein and diastolic dysfunction, improving the identification of the best ventilator settings, minimizing detrimental hemodynamic effects secondary to the use of elevated PEEP levels (38). Studies on animal models suggest that LUS can be useful in early diagnosis of ARDS, as B-patterns can be seen also during the exudative phase of ARDS, likely initial expression of extravascular lung water accumulation, when CXR has particularly low sensitivity (39). A strong correlation between quantitative LUS grayscale analysis and EVLW density in isolated bovine lungs (40). This could improve early diagnosis of ARDS, potentially promoting a prompt implementation of protective ventilatory strategies.

Another potential role of LUS is the monitoring of ARDS progression and the effects of ventilation settings. The loss of aeration and its regional distribution can be estimated with LUS (33,41) through the attribution of numeric values at each LUS pattern. Thereafter, various algorithms have been created to use LUS as a tool for the respiratory monitoring and diagnostic of critically ill patients (42). Score-based LUS can assess aeration or changes in aeration semi-quantitatively in different thoracic districts, allowing a better understanding of the lung morphology and the distribution of focal or diffuse

aeration loss in the early phases of ARDS (41). A score based on the examination of predefined chest regions use was studied, validated and applied in different aspects of the management of the ARDS patient, including PEEP titration (43), response to recruitment manoeuvres (44), prone positioning (45) and during the weaning phase (46).

In conclusion, LUS is non-invasive, available at the bedside, reproducible, inexpensive, and does not require ionizing radiation. However, it cannot identify lung overinflation, it is difficult to use in obese patients, in subjects with alterations of the rib cage subcutaneous emphysema or surgical dressings, due to non-optimal acoustic windows. In addition, this is an operator-dependent technique, although characterized by a steep learning curve and a good intra and inter-observer agreement (41).

EIT

Lung EIT is a non-invasive, radiation-free technique that quantifies relative changes in lung tissue aeration during breathing and reconstructs images based on the distribution of ventilation at the bedside (47). It is based on the physical principle that changes in lung gas content modify its impedance: lung resistivity depends on anatomy, gas and air content, amount of intracellular and extracellular fluids and blood content. Therefore, during mechanical ventilation, lung impedance depends strictly on the degree of inflation. Non-ventilated parenchyma yields no signal in EIT scans, as its electrical impedance does not vary throughout the respiratory cycle. Commercially available EIT scanners have a low spatial resolution on the axial plane, and images are representative of the impedance changes in a thorax cross-section of about 5 to 10 cm (48). EIT has been validated as a tool to estimate several respiratory parameters, such as the end-expiratory lung volume versus nitrogen washout test and plethysmography (49), and the distribution of lung volumes compared to CT (50). EIT can also provide indirect quantification of lung perfusion, either measuring the signal pulsatility due to the blood flow, or temporarily increasing the conductance of perfused lung areas with an injection of hypertonic saline in a central venous line (51).

In ARDS patients, EIT can visualize directly and non-invasively the effects of mechanical ventilation at the bedside, potentially helping the clinician to titrate ventilation parameters (52,53). In ARDS, interstitial oedema increases the effects of gravity dependent lung regions, and EIT can detect such loss of aeration along with compensatory increases in ventilation of ventral regions

(49,50,53). In mechanically ventilated patients, EIT can detect differences in regional ventilation reflecting the extension of lung injury and the effects of ventilation, including the application of PEEP (52-54) and recruitment manoeuvres (55) and tidal volume. Moreover, EIT can be used to calculate regional compliance during titration of PEEP and to distinguish non-recruited lung tissue from the recruited one (50). In mechanically ventilated ARDS patients, hyperdistention mainly occurs in ventral regions, and results in an elevated impedance that can be detected by EIT. However, since the signal does not vary throughout the respiratory cycle, the EIT monitor shows a silent area, as occurs in non-aerated regions. The distinction between the two entities is based on a topographic evaluation. Nonetheless, recent studies tried to use EIT to map local pressure/volume curves to detect tidal recruitment and overdistension (56). Several EIT-based protocols have been proposed to guide the setting of PEEP during mechanical ventilation in ARDS, including patients receiving extracorporeal membrane lung oxygenation (57). However, the impact of these approaches on clinical outcome is not yet demonstrated.

In conclusion, EIT is a new and developing technique, still affected by several technical pitfalls, including low spatial resolution, susceptibility to interferences from other medical devices used in the ICU, and the need for assuming a standard chest shape to reconstruct images in real-time (58). It is likely that this technique will be further developed in the next years, possibly providing additional tools to optimise the management of ARDS patients.

Techniques under development

This section will briefly address two techniques that have been proposed, so far mainly in the research context, to provide additional information on the respiratory function in ARDS patients. It is the case of positron emission tomography (PET) and magnetic resonance imaging (MRI).

PET

PET is a functional imaging technique based on the detection of a radioactive tracer on a biologically active molecule administered to patients, and has recently been used both in clinical and experimental studies to investigate ARDS (43). It can quantify regional perfusion, ventilation, aeration, oedema, lung vascular permeability, metabolic activity of inflammatory cells, enzyme activity and

pulmonary gene expression (59,60).

Differently from morphological imaging, PET gives additional functional information about the injured lung. Despite the well-known presence of a ventro-dorsal aeration gradient in ARDS, PET clarified that the increase in vascular permeability is homogeneously distributed in the whole lung (61), namely showing that also regions that had normal density at the CT were interested by the pathological process. Furthermore, PET measurements of regional perfusion in ARDS revealed that patients with similar extension of lung opacities can have different $\text{PaO}_2/\text{FiO}_2$ ratios and disease severity (62), according to the redistribution of the perfusion away from non-aerated regions resulting in different shunt fractions. PET-based perfusion measurements also clarified the mechanism underlying the paradoxical decrease in oxygenation sometimes seen after performing recruitment manoeuvres: in addition to recruitment, perfusion can be diverted from regions towards the de-recruited lung, worsening the ventilation/perfusion matching (63). Another study using ^{68}Ga -marked albumin aggregates suggested also that, in the early stages of lung injury, perfusion is redistributed towards healthier regions due to hypoxic vasoconstriction or direct compression of vessels by oedema (64).

PET performed with [^{18}F]fluoro-2-deoxy-D-glucose (FDG) has been extensively used in research to quantify regional lung inflammation in ARDS (60): activated neutrophils have a higher glucose metabolism compared with other inflammatory cells in lung because their metabolism is mostly based on anaerobic glycolysis. Many studies highlighted an enhanced metabolic activity in the ARDS lung, either in the consolidated areas or normal density areas, and the metabolic activity of inflammatory cells in normal parenchyma may be consequent to the effects of mechanical ventilation, mainly exerted on aerated regions. The [^{18}F]-FDG uptake is directly proportional to the regional tidal volume normalized by end-expiratory lung volume and increases after administration of plateau airway pressures higher than 27 cmH_2O (65). Other studies showed a linear correlation between regional lung volumetric strain, respiratory gating of inhaled $^{13}\text{N}_2$ PET scans and the velocity of phosphorylation of [^{18}F]-FDG, that has been correlated to the increase of pro-inflammatory cytokines as IL-1 β , IL-8 and IL-10 in experimental ARDS (66). In a study on a porcine model of ARDS, PET compared the inflammatory response due to atelectrauma compared to volutrauma, with the latter being significantly more relevant (23), suggesting extreme caution in applying the

elevated PEEP levels required to achieve an open lung strategy (22).

PET is unlikely to become a routine diagnostic tool, due to its low availability, high cost and high radiation exposure, but it could be useful in selected cases. However, its ability to provide functional and biological information *in vivo* its role in research is hardly replaceable.

MRI

MRI is another functional technique that provides the opportunity to study the pathophysiology of pulmonary disease. Its application to the lung has been limited due to technical restrictions such as the slowness of image acquisition limiting the possibility to scan the chest during a breath-hold, the low proton density in the lung, about $1/5^{\text{th}}$ of signal-generating protons compared to other solid organs (67) and the fast signal decay due to susceptibility to artefacts at air-tissue interfaces (68). Thanks to the recent technical advances and the availability of single breath-hold fast sequences, lung MRI could become a radiation-free alternative to CT.

Air has no protons but lung parenchyma generates little MRI signal that can be compared to other signals of solid organs or structures present in the mediastinum. Proton density per voxel is determined by the lung inflation and consequently, by lung aeration status. Within the same individual, changes in lung volume will cause equal changes in proton density and, accordingly, equal changes in MR signal intensity of the lung parenchyma (69). Hyperpolarized gas MRI was used to evaluate alveolar recruitment and atelectasis-induced overdistension during mechanical ventilation in ARDS (70). Helium-3 and Xenon-129 (71) can be used as contrast agents due to their capacity of diffusing rapidly into airspaces and enabling detection of ventilated lung tissue (72). Hyperpolarized Xenon-129 follows the same pathway as oxygen, it spreads across the alveolocapillary membrane allowing the calculation of gas exchange parameters, including alveolar surface area, septal thickness and vascular transit time (72,73). MRI enables calculation of alveolar size based on the MRI apparent diffusion coefficient (73), and this has a potential application to determine the consequences of atelectasis and recruitment manoeuvres (70). Gases with fast spin-rotation relaxation at thermal equilibrium polarization have been used to study differences in ventilation-perfusion ratio (74) and time constants for fast and slow filling lung compartments, giving information

about ventilation-perfusion heterogeneity, pulmonary end-capillary diffusion of oxygen and lung microstructure in ARDS (75). Visualization of ventilation is also possible using oxygen-enhanced MRI (72). MR lung tissue imaging was used to image the elastic properties of lungs with ventilator-induced lung injury in rats (76) and to study the physiopathology and the progress of lung injury. Furthermore, morphological and pathophysiological patterns like 'ground-glass opacification' and 'consolidation' in ARDS could be detected by MRI similarly as with CT (75). A recent work in rats demonstrated that lung MRI can detect small regions of ventilator-induced injury earlier than the appearance of alterations in lung mechanics in rats, this finding was confirmed with histology and the authors also demonstrated the possibility of visualizing and quantifying the regression of injury in real-time, after adoption of protective mechanical ventilation strategies (77).

The strength of MRI lies in the absence of radiations, the ability to perform functional imaging, estimating perfusion and respiratory mechanics. It also has a variety of contrast mechanisms that may help to distinguish cellular inflammation, atelectasis and oedema. Further clinical research is warranted to translate these experimental findings in useful tools for the diagnosis and management of ARDS.

Conclusions

ARDS still has a high mortality, and is associated with elevated morbidity, length of stay and healthcare cost, and CT remains the gold standard technique to make diagnosis and monitor its evolution. CXR is still commonly performed despite its limited specificity, while LUS and EIT are emerging bedside tools, playing an important role in the ICU setting. PET and MRI are now mainly used for research purpose and might have a role in selected cases. Despite the important pathophysiological information derived from imaging, further research is warranted to standardise the role of different techniques in the management of ARDS patients.

Acknowledgements

None.

Footnote

Conflicts of Interest: The authors have no conflicts of interest

to declare.

References

1. ARDS Definition Task Force, Ranieri VM, Rubenfeld GD, et al. Acute respiratory distress syndrome: the Berlin Definition. *JAMA* 2012;307:2526-33.
2. Bellani G, Laffey JG, Pham T, et al. Epidemiology, Patterns of Care, and Mortality for Patients With Acute Respiratory Distress Syndrome in Intensive Care Units in 50 Countries. *JAMA* 2016;315:788-800.
3. Bernard GR, Artigas A, Brigham KL, et al. The American-European Consensus Conference on ARDS. Definitions, mechanisms, relevant outcomes, and clinical trial coordination. *Am J Respir Crit Care Med* 1994;149:818-24.
4. Thompson BT, Guérin C, Esteban A. Should ARDS be renamed diffuse alveolar damage? *Intensive Care Med* 2016;42:653-5.
5. Eisenhuber E, Schaefer-Prokop CM, Prosch H, et al. Bedside chest radiography. *Respir Care* 2012;57:427-43.
6. Sheard S, Rao P, Devaraj A. Imaging of Acute Respiratory Distress Syndrome. *Respir Care* 2012;57:607-12.
7. Bombino M, Gattinoni L, Pesenti A, et al. The value of portable chest roentgenography in adult respiratory distress syndrome. Comparison with computed tomography. *Chest* 1991;100:762-9.
8. Figueroa-Casas JB, Brunner N, Dwivedi AK, et al. Accuracy of the chest radiograph to identify bilateral pulmonary infiltrates consistent with the diagnosis of acute respiratory distress syndrome using computed tomography as reference standard. *J Crit Care* 2013;28:352-7.
9. Zompatori M, Ciccarese F, Fasano L. Overview of current lung imaging in acute respiratory distress syndrome. *Eur Respir Rev* 2014;23:519-30.
10. Wallet F, Delannoy B, Haquin A, et al. Evaluation of Recruited Lung Volume at Inspiratory Plateau Pressure With PEEP Using Bedside Digital Chest X-ray in Patients With Acute Lung Injury/ARDS. *Respir Care* 2013;58:416-23.
11. Peng JM, Qian CY, Yu XY, et al. Does training improve diagnostic accuracy and inter-rater agreement in applying the Berlin radiographic definition of acute respiratory distress syndrome? A multicenter prospective study. *Crit Care* 2017;21:12.
12. Gattinoni L, Caironi P, Pelosi P, et al. What has computed tomography taught us about the acute respiratory distress syndrome? *Am J Respir Crit Care Med* 2001;164:1701-11.
13. Mull RT. Mass estimates by computed tomography: physical density from CT numbers. *AJR Am J Roentgenol* 1984;143:1101-4.
14. Gattinoni L, Mascheroni D, Torresin A, et al. Morphological response to positive end expiratory pressure in acute respiratory failure. Computerized tomography study. *Intensive Care Med* 1986;12:137-42.
15. Ball L, Sutherasan Y, Pelosi P. Monitoring respiration: What the clinician needs to know. *Best Pract Res Clin Anaesthesiol* 2013;27:209-23.
16. Gattinoni L, Pesenti A. The concept of "baby lung." *Intensive Care Med* 2005;31:776-84.
17. Petrucci N, De Feo C. Lung protective ventilation strategy for the acute respiratory distress syndrome. *Cochrane Database Syst Rev* 2013;(2):CD003844.
18. Briel M, Meade M, Mercat A, et al. Higher vs Lower Positive End-Expiratory Pressure in Patients With Acute Lung Injury and Acute Respiratory Distress Syndrome: Systematic Review and Meta-analysis. *JAMA* 2010;303:865-73.
19. Gattinoni L, Caironi P, Cressoni M, et al. Lung recruitment in patients with the acute respiratory distress syndrome. *N Engl J Med* 2006;354:1775-1786.
20. Pelosi P, Rocco PR, de Abreu MG. Use of computed tomography scanning to guide lung recruitment and adjust positive-end expiratory pressure. *Curr Opin Crit Care* 2011;17:268-74.
21. Chiumello D, Marino A, Brioni M, et al. Visual anatomical lung CT scan assessment of lung recruitability. *Intensive Care Med* 2013;39:66-73.
22. Cressoni M, Chiumello D, Algieri I, et al. Opening pressures and atelectrauma in acute respiratory distress syndrome. *Intensive Care Med* 2017;43:603-11.
23. Güldner A, Braune A, Ball L, et al. Comparative Effects of Volutrauma and Atelectrauma on Lung Inflammation in Experimental Acute Respiratory Distress Syndrome. *Crit Care Med* 2016;44:e854-65.
24. Ball L, Brusasco C, Corradi F, et al. Lung hyperaeration assessment by computed tomography: correction of reconstruction-induced bias. *BMC Anesthesiol* 2016;16:67.
25. Reske AW, Reske AP, Gast HA, et al. Extrapolation from ten sections can make CT-based quantification of lung aeration more practicable. *Intensive Care Med* 2010;36:1836-44.
26. Vecchi V, Langer T, Bellomi M, et al. Low-dose CT for quantitative analysis in acute respiratory distress syndrome. *Crit Care* 2013;17:R183.
27. Ball L, Braune A, Corradi F, et al. Ultra-low-dose

- sequential computed tomography for quantitative lung aeration assessment—a translational study. *Intensive Care Med Exp* 2017;5:19.
28. Reske AW, Rau A, Reske AP, et al. Extrapolation in the analysis of lung aeration by computed tomography: a validation study. *Crit Care* 2011;15:R279.
 29. Reich H, Moens Y, Braun C, et al. Validation study of an interpolation method for calculating whole lung volumes and masses from reduced numbers of CT-images in ponies. *Vet J Lond Engl* 1997 2014;202:603-7.
 30. Chiumello D, Langer T, Vecchi V, et al. Low-dose chest computed tomography for quantitative and visual anatomical analysis in patients with acute respiratory distress syndrome. *Intensive Care Med* 2014;40:691-9.
 31. Via G, Storti E, Gulati G, et al. Lung ultrasound in the ICU: from diagnostic instrument to respiratory monitoring tool. *Minerva Anesthesiol* 2012;78:1282-96.
 32. Gargani L, Volpicelli G. How I do it: lung ultrasound. *Cardiovasc Ultrasound* 2014;12:25.
 33. Volpicelli G, Elbarbary M, Blaivas M, et al. International evidence-based recommendations for point-of-care lung ultrasound. *Intensive Care Med* 2012;38:577-91.
 34. Lichtenstein DA, Lascols N, Mezière G, et al. Ultrasound diagnosis of alveolar consolidation in the critically ill. *Intensive Care Med* 2004;30:276-81.
 35. Agricola E, Bove T, Oppizzi M, et al. “Ultrasound comet-tail images”: a marker of pulmonary edema: a comparative study with wedge pressure and extravascular lung water. *Chest* 2005;127:1690-5.
 36. Papazian L, Calfee CS, Chiumello D, et al. Diagnostic workup for ARDS patients. *Intensive Care Med* 2016;42:674-85.
 37. Riviello ED, Kiviri W, Twagirumugabe T, et al. Hospital Incidence and Outcomes of the Acute Respiratory Distress Syndrome Using the Kigali Modification of the Berlin Definition. *Am J Respir Crit Care Med* 2016;193:52-9.
 38. Lazzeri C, Cianchi G, Bonizzoli M, et al. The potential role and limitations of echocardiography in acute respiratory distress syndrome. *Ther Adv Respir Dis* 2016;10:136-48.
 39. Gargani L, Lionetti V, Di Cristofano C, et al. Early detection of acute lung injury uncoupled to hypoxemia in pigs using ultrasound lung comets. *Crit Care Med* 2007;35:2769-74.
 40. Corradi F, Ball L, Brusasco C, et al. Assessment of extravascular lung water by quantitative ultrasound and CT in isolated bovine lung. *Respir Physiol Neurobiol* 2013;187:244-9.
 41. Bellani G, Rouby JJ, Constantin JM, et al. Looking closer at acute respiratory distress syndrome: the role of advanced imaging techniques. *Curr Opin Crit Care* 2017;23:30-7.
 42. Bouhemad B, Mongodi S, Via G, et al. Ultrasound for “lung monitoring” of ventilated patients. *Anesthesiology* 2015;122:437-47.
 43. Luecke T, Corradi F, Pelosi P. Lung imaging for titration of mechanical ventilation. *Curr Opin Anaesthesiol* 2012;25:131-40.
 44. Bouhemad B, Brisson H, Le-Guen M, et al. Bedside Ultrasound Assessment of Positive End-Expiratory Pressure-induced Lung Recruitment. *Am J Respir Crit Care Med* 2011;183:341-7.
 45. Haddam M, Zieleskiewicz L, Perbet S, et al. Lung ultrasonography for assessment of oxygenation response to prone position ventilation in ARDS. *Intensive Care Med* 2016;42:1546-56.
 46. Mayo P, Volpicelli G, Lerolle N, et al. Ultrasonography evaluation during the weaning process: the heart, the diaphragm, the pleura and the lung. *Intensive Care Med* 2016;42:1107-17.
 47. Moerer O, Hahn G, Quintel M. Lung impedance measurements to monitor alveolar ventilation: *Curr Opin Crit Care* 2011;17:260-7.
 48. Adler A, Amato MB, Arnold JH, et al. Whither lung EIT: Where are we, where do we want to go and what do we need to get there? *Physiol Meas* 2012;33:679-94.
 49. Costa ELV, Lima RG, Amato MB. Electrical impedance tomography. *Curr Opin Crit Care* 2009;15:18-24.
 50. Victorino JA, Borges JB, Okamoto VN, et al. Imbalances in Regional Lung Ventilation: A Validation Study on Electrical Impedance Tomography. *Am J Respir Crit Care Med* 2004;169:791-800.
 51. Borges JB, Suarez-Sipmann F, Bohm SH, et al. Regional lung perfusion estimated by electrical impedance tomography in a piglet model of lung collapse. *J Appl Physiol* 2012;112:225-36.
 52. Mauri T, Bellani G, Confalonieri A, et al. Topographic Distribution of Tidal Ventilation in Acute Respiratory Distress Syndrome: Effects of Positive End-Expiratory Pressure and Pressure Support*. *Crit Care Med* 2013;41:1664-73.
 53. Cinnella G, Grasso S, Raimondo P, et al. Physiological Effects of the Open Lung Approach in Patients with Early, Mild, Diffuse Acute Respiratory Distress Syndrome: An Electrical Impedance Tomography Study. *Anesthesiology* 2015;123:1113-21.
 54. Hochhausen N, Biener I, Rossaint R, et al. Optimizing

- PEEP by Electrical Impedance Tomography in a Porcine Animal Model of ARDS. *Respir Care* 2017;62:340-9.
55. Dargaville PA, Rimensberger PC, Frerichs I. Regional tidal ventilation and compliance during a stepwise vital capacity manoeuvre. *Intensive Care Med* 2010;36:1953-61.
 56. Beda A, Carvalho AR, Carvalho NC, et al. Mapping Regional Differences of Local Pressure-Volume Curves With Electrical Impedance Tomography: *Crit Care Med* 2017;45:679-86.
 57. Franchineau G, Bréchet N, Lebreton G, et al. Bedside Contribution of Electrical Impedance Tomography to Set Positive End-Expiratory Pressure for ECMO-Treated Severe ARDS Patients. *Am J Respir Crit Care Med* 2017. [Epub ahead of print].
 58. Grychtol B, Lionheart WR, Bodenstern M, et al. Impact of Model Shape Mismatch on Reconstruction Quality in Electrical Impedance Tomography. *IEEE Trans Med Imaging* 2012;31:1754-60.
 59. Chen DL, Cheriyan J, Chilvers ER, et al. Quantification of Lung PET Images: Challenges and Opportunities. *J Nucl Med* 2017;58:201-7.
 60. Bellani G, Amigoni M, Pesenti A. Positron emission tomography in ARDS: a new look at an old syndrome. *Minerva Anestesiol* 2011;77:439-47.
 61. Sandiford P, Province MA, Schuster DP. Distribution of Regional Density and Vascular Permeability in the Adult Respiratory Distress Syndrome. *Am J Respir Crit Care Med* 1995;151:737-42.
 62. Schuster DP, Anderson C, Kozlowski J, et al. Regional Pulmonary Perfusion in Patients with Acute Pulmonary Edema. *J Nucl Med* 2002;43:863-70.
 63. Musch G, Harris RS, Vidal Melo MF, et al. Mechanism by Which a Sustained Inflation Can Worsen Oxygenation in Acute Lung Injury. *Anesthesiology* 2004;100:323-30.
 64. Richter T, Bergmann R, Musch G, et al. Reduced pulmonary blood flow in regions of injury 2 hours after acid aspiration in rats. *BMC Anesthesiol* 2015;15:36.
 65. Bellani G, Guerra L, Musch G, et al. Lung Regional Metabolic Activity and Gas Volume Changes Induced by Tidal Ventilation in Patients with Acute Lung Injury. *Am J Respir Crit Care Med* 2011;183:1193-9.
 66. de Prost N, Feng Y, Wellman T, et al. 18F-FDG Kinetics Parameters Depend on the Mechanism of Injury in Early Experimental Acute Respiratory Distress Syndrome. *J Nucl Med* 2014;55:1871-7.
 67. Mulkern R, Haker S, Mamata H, et al. Lung Parenchymal Signal Intensity in MRI: A Technical Review with Educational Aspirations Regarding Reversible Versus Irreversible Transverse Relaxation Effects in Common Pulse Sequences. *Concepts Magn Reson Part A Bridg Educ Res* 2014;43A:29-53.
 68. Biederer J, Mirsadraee S, Beer M, et al. MRI of the lung (3/3)—current applications and future perspectives. *Insights Imaging* 2012;3:373-86.
 69. Bankier AA, O'Donnell CR, Mai VM, et al. Impact of lung volume on MR signal intensity changes of the lung parenchyma. *J Magn Reson Imaging* 2004;20:961-6.
 70. Cereda M, Emami K, Kadlecsek S, et al. Quantitative imaging of alveolar recruitment with hyperpolarized gas MRI during mechanical ventilation. *J Appl Physiol* 2011;110:499-511.
 71. Ebner L, Kammerman J, Driehuis B, et al. The role of hyperpolarized ^{129}Xe in MR imaging of pulmonary function. *Eur J Radiol* 2017;86:343-52.
 72. Matsuoka S, Hunsaker AR, Gill RR, et al. Functional MR Imaging of the Lung. *Magn Reson Imaging Clin N Am* 2008;16:275-89, ix.
 73. Emami K, Stephen M, Kadlecsek S, et al. Quantitative Assessment of Lung Using Hyperpolarized Magnetic Resonance Imaging. *Proc Am Thorac Soc* 2009;6:431-8.
 74. Adolphi NL, Kuethe DO. Quantitative mapping of ventilation-perfusion ratios in lungs by ^{19}F MR imaging of T_1 of inert fluorinated gases. *Magn Reson Med* 2008;59:739-46.
 75. Chiumello D, Froio S, Bouhemad B, et al. Clinical review: Lung imaging in acute respiratory distress syndrome patients - an update. *Crit Care* 2013;17:243.
 76. McGee KP, Mariappan YK, Hubmayr RD, et al. Magnetic resonance assessment of parenchymal elasticity in normal and edematous, ventilator-injured lung. *J Appl Physiol* 2012;113:666.
 77. Kuethe DO, Filipeczak PT, Hix JM, et al. Magnetic Resonance Imaging Provides Sensitive In Vivo Assessment of Experimental Ventilator-Induced Lung Injury. *Am J Physiol Lung Cell Mol Physiol* 2016;311:L208-18.

Cite this article as: Ball L, Vercesi V, Costantino F, Chandrapatham K, Pelosi P. Lung imaging: how to get better look inside the lung. *Ann Transl Med* 2017;5(14):294. doi: 10.21037/atm.2017.07.20